Design of AC Resonant Inductors Using Area Product Method

Marian K. Kazimierczuk† Hiroo Sekiya†‡
†Department of Electrical Engineering, Wright State University, Dayton, Ohio, 45435-0001 USA
‡Graduate School of Advanced Integration Science, Chiba University, Chiba, 263–8522, JAPAN
Email: marian.kazimierczuk@wright.edu sekiya@faculty.chiba-u.jp

***Abstract*—There are no well-established criteria for selecting the core for the design of resonant inductors. This paper presents new expressions of the area product for resonant inductors. By using proposed expressions, the area-product value can be calculated from loaded-quality factor of a resonant circuit, output power, and operating frequency assuming the window utilization factor and the maximum flax density. The area-product value expressed in terms of the loaded-quality factor is a good criterion for selecting the core. The design examples are given for single-wire winding and multiple-strand winding with a gapped core taking into account skin, proximity, and fringing effects.**

***Index Terms*—inductor design, area product method, resonant inductor, skin effect, multiple strands, proximity effect, fringing effect**

I. Introduction

The inductor design is a traditional problem, but it is not solved satisfactorily in the power electronics field. There are several design procedures for designingful resonant inductors [1] – [3]. However, these methods have no well-established criteria for selecting a core made by different manufactures for resonant inductors. The iterative process is needed to select a core. There are several well-known strategies for selecing a core, for example, an area product (A_p) method [4]–[8] and core geometry (K_g) method [7], [8]. These methods are primarily used in the design of inductors and transformers for switching-mode power supplies. The concept of the A_p approach is to select a proper core satisfying both the electromagnetic conditions and the restriction of the core window area. The inductance value is adjusted by the gap length. The A_p method is widely used for designing the inductors and transformers for dc-dc power converters operating in CCM and DCM.

This paper presents new expressions for the area product for resonant inductors. By using the proposed expressions, we can determine the area-product value from loaded-quality factor, output power, and operating frequency, assuming the window utilization factor and the maximum flax density. The area product value is a good criterion to select the core. The design examples are given for single-wire winding and multiple-strand winding with a gapped core taking into account skin, proximity, and fringing effects.

II. Derivation of Core Area Product A_p for Sinusoidal Inductor Current and Voltage Waveforms

We assume that the inductor current and voltage waveforms are sinusoidal with angular frequency $\omega = 2\pi f$. The amplitude of a sinusoidal voltage across an inductor with N turns of wire is given by

$$V_m = \omega N \phi_m = \omega N A_c B_m, \tag{1}$$

where A_c, ϕ, and B_m are the cross-sectional area of a magnetic core, the amplitude of a magnetic flux in the core, and the amplitude of a magnetic flax density in the core, respectively. The number of turns of the inductor for a sinusoidal inductor voltage waveform is

$$N = \frac{V_m}{\omega A_c B_m} = \frac{L I_m}{A_c B_m}, \tag{2}$$

where L and I_m are the inductance and the amplitude of a sinusoidal current through the inductor. For fixed values of L, I_m, and B_m, the number of turns N is governed by the core cross-sectional area A_c. The amplitude in the current density of the winding conductor is

$$J_m = \frac{I_m}{A_w}, \tag{3}$$

where A_w is the cross-sectional area of the winding wire. For a round wire of bare conductor diameter d,

$$A_w = \frac{\pi d^2}{4}. \tag{4}$$

A core window must provide sufficient space for a winding in a bobbin (if any). The cross-sectional area of a core window must provide enough space for bare wire insulation, and air space between the insulated wire turns. The window utilization factor is defined as the ratio of the total conductor (copper) cross-sectional area NA_w to the total window area W_a

$$K_u \equiv \frac{N A_w}{W_a} = \frac{N I_m}{W_a J_m}. \tag{5}$$

Wire insulation area, air area, bobbin area, and wire lay (fill factor) reduce the value of the window utilization factor K_u to less than 1. The typical values of K_u are from 0.3 to 0.7 [7]. From (5), the number of the wire turns is also obtained as

$$N = \frac{K_u W_a J_m}{N I_m}. \tag{6}$$

978-1-4244-2893-9/09/$25.00 ©2009 IEEE

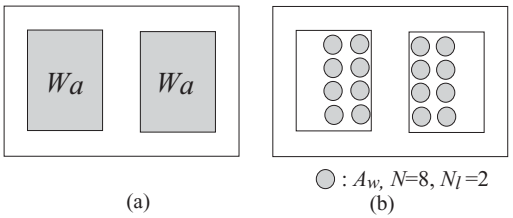

Fig. 1. Winding window of EE core. (a) Window cross-sectional area W_a. (b) Window utilization factor $K_u = NA_w/W_a$.

For fixed values of K_u, I_m, and J_m, the number of turns N is determined by the total window area. Figure 1 illustrates a winding window for an EE core. The core window area W_a is related to the conduction (copper) area, and hence the current capability of an inductor.

Equating the right-hand sides of (2) and (5), the *area product* is obtained as

$$A_p = W_a A_c = \frac{A_w L I_m}{K_u B_m} = \frac{L I_m^2}{K_u J_m B_m} = \frac{2W_m}{K_u J_m B_m}, \quad (7)$$

where the energy stored in the inductor is

$$W_m = \frac{1}{2} L I_m^2. \quad (8)$$

and the apparent power of the inductor is

$$P_Q = \frac{1}{2} I_m V_m = f W_m. \quad (9)$$

The area product A_p indicates the core with a good combination of W_a and A_c satisfying the number of turns from electromagnetic conditions in (2) and from the core-window-area restriction in (5) simultaneously. It is quoted by many manufacturers or can be calculated from the core dimensions. The left-hand side of the expression for A_p contains the mechanical core parameters and the right-hand side of the expressions includes the inductor electrical parameters. The core cross-sectional area A_c is related to the magnetic flux conduction capability. The window area W_a is related to the current conduction capability.

Generally, the loaded quality factor of a series-resonant L-C-R circuit shown in Fig. 2(a) is defined as

$$\begin{aligned} Q_L &= \frac{\omega L}{R} = \frac{\omega L I_m^2}{2P_o} \\ &= \frac{\omega W_m}{P_o} \\ &= \frac{2\pi f W_m}{P_o}. \end{aligned} \quad (10)$$

$P_o = I_m^2/2$, yielding $R = 2P_o/I_m^2$ is the output power of a resonant circuit. For parallel-resonant L-C-R circuit as shown in Fig. 2(b), the loaded quality factor is defined as

$$Q_L = \frac{R}{\omega L}. \quad (11)$$

The relationship between the amplitude of the current through the resonant inductor I_m and that through the output resistance

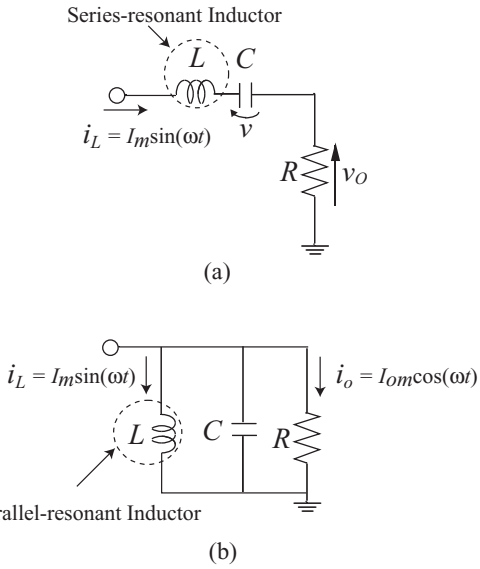

Fig. 2. Resosnant circuit. (a) Series-resonant circuit. (b) Parallel resonant circuit.

I_{om} is

$$I_m = Q_L I_{om}. \quad (12)$$

The output power of the resonant circuit is

$$P_o = \frac{2I_{om}^2}{2} = R I_m^2 2Q_L^2, \quad (13)$$

yielding the load resistance

$$R = \frac{2Q_L^2 P_o}{I_m^2}. \quad (14)$$

Therefore, (11) is rewritten as

$$Q_L = \frac{R}{\omega L} = \frac{2Q_L^2 P_o}{\omega L I_m^2} = \frac{Q_L^2 P_o}{\omega W_m}. \quad (15)$$

Finally, we obtain

$$\begin{aligned} Q_L &= \frac{\omega W_m}{P_o} \\ &= \frac{2\pi f W_m}{P_o}. \end{aligned} \quad (16)$$

From (10) and (16), it is seen that the relationship between Q_L and W_m for the parallel-resonant circuit is the same as that for the series-resonant circuit. Thus, the area product for resonant inductors is given by

$$\begin{aligned} A_p &= W_a A_c \\ &= \frac{2W_m}{K_u J_m B_m} \\ &= \frac{2Q_L P_o}{\omega K_u J_m B_m} \\ &= \frac{2Q_L P_o}{\pi f K_u J_m B_m}. \end{aligned} \quad (17)$$

The expressions for the area product A_p for resonant inductors given by (7) and (17) are proposed in this paper, which

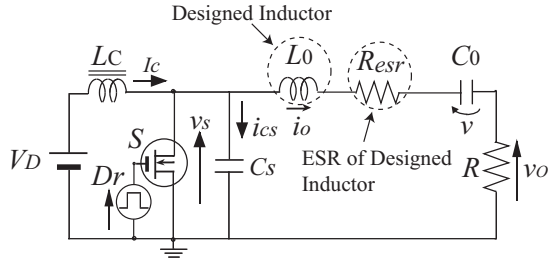

Fig. 3. Circuit topology of the class E amplifier.

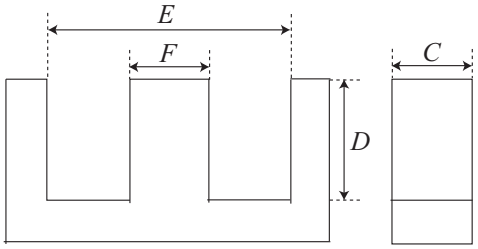

Fig. 4. Mechanical dimensions of E core.

are valid for both the series-resonant inductor and the parallel-resonant one. The resonant inductors are required to store the large amount of magnetic energy, which require a high loaded quality factor. Typically, the loaded-quality factor Q_L is greater than 5.

III. Design Example

This section gives a design example of a resonant inductor for the class E resonant power amplifier whose topology is shown in Fig. 3. We design the resonant inductor L_0 to meet the following specifications: $f = 100$ kHz, $P_o = 80$ W, $R = 70\ \Omega$, and $Q_L = 5$. From these specifications, we obtain

$$I_m = \sqrt{2P_o/R} = 1.51 \text{ A} \tag{18}$$

and

$$L_0 = Q_L R/\omega = 557\ \mu\text{H}. \tag{19}$$

Additionally, we assume the following: $J_m < 5$ A/mm^2, $K_u = 0.4$, and $B_m = 0.2$ T. From (17), the required area product of the inductor is

$$\begin{aligned} A_p &= \frac{2Q_L P_o}{\omega K_u J_m B_m} \\ &= \frac{2 \times 7 \times 80}{2 \times \pi \times 100 \times 10^3 \times 0.4 \times 5 \times 10^6 \times 0.2}\ (\text{m}^4) \\ &= 0.398\ \text{cm}^4. \end{aligned} \tag{20}$$

We shall choose a Magnetics 0F-42515EC ferrite EE core with the following parameters [9]: $A_p = 0.42$ cm^4, $A_c = 40.1$mm^2, $l_c = 73.5$ mm, $V_c = 2.95$ cm^3, and $B_s = 0.5$ T, where l_c, V_c, and B_s and are the core length, the saturated flux density, and the core volume, respectively. The core dimensions C, D, E, and F, which are defined as shown in Fig. 4, are $C = F = 6.35 \pm 0.25$ mm, $D = 12.6$ mm, and $E = 18.8$ mm (in minimum). We also choose a Magnetics bobbin 00B251501 [9]. The height of the bobbins is $H = 20.57$ mm. The core is made of the F-type material whose relative permeability $\mu_r = 3000 \pm 20\ \%$. The core loss per unit volume P_v of this type of material is given by

$$\begin{aligned} P_v &= af^c(10 \times B_m)^d \\ &= \begin{cases} 0.790 \times f^{1.06} \times (10 \times B_m)^{2.85} \\ \quad \text{for } f < 10 \text{ kHz} \\ 0.0717 \times f^{1.72} \times (10 \times B_m)^{2.66} \\ \quad \text{for } 10 \text{ kHz} \le f < 100 \text{ kHz} \\ 0.0573 \times f^{1.66} \times (10 \times B_m)^{2.68} \\ \quad \text{for } 100 \text{ kHz} \le f < 500 \text{ kHz} \\ 0.0126 \times f^{1.88} \times (10 \times B_m)^{2.29} \\ \quad \text{for } f \ge 500 \text{ kHz}, \end{cases} \end{aligned} \tag{21}$$

where f is in kHz, B_m is in T, and P_v is in mW/cm^3.

The core winding window area is

$$\begin{aligned} W_a &= \frac{A_p}{A_c} \\ &= \frac{0.42 \times 10^{-8}}{0.401 \times 10^{-6}}\ (\text{m}^2) = 104\ \text{mm}^2. \end{aligned} \tag{22}$$

We consider two kinds of designs, one is the design with a single-wire winding and the other is that with a multiple-strand winding.

A. Single-Wire Winding

The cross-sectional area of the winding bare wire is

$$\begin{aligned} A_w &= \frac{I_m}{J_m} \\ &= \frac{1.51}{4 \times 10^6}\ (\text{m}^2) = 0.378\ \text{mm}^2. \end{aligned} \tag{23}$$

An AWG 21 copper wire with $A_w = 0.411$ mm^2 and a bare wire diameter $d = 0.723$ mm is selected. The amplitude of the current density is

$$\begin{aligned} J_m &= \frac{I_m}{A_w} \\ &= \frac{1.51}{0.411 \times 10^{-6}}\ (\text{A/m}^2) = 3.68\ \text{A/mm}^2, \end{aligned} \tag{24}$$

which satisfies the inductor specification of J_m. Because the nominal outer diameter of the AWG 21 wire is $d_o = 0.785$ mm, the number of turns is obtained from (5):

$$\begin{aligned} N &= \frac{K_u W_a}{A_w} \cdot \frac{K_u W_a}{\pi d^2/4} \\ &= \frac{0.4 \times 104.7}{\pi \times 0.723^2/4} = 102.0 \text{ turns}. \end{aligned} \tag{25}$$

We pick $N = 102$ turns. For the adjustment of the inductance L_0, the air-gap length is calculated as

$$\begin{aligned} l_g &= \frac{\mu_0 A_c N^2}{L_0} - \frac{l_c}{\mu_r} \\ &= \frac{4 \times \pi \times 10^{-7} \times 40.1 \times 10^{-6} \times 102^2}{557 \times 10^{-6}} \\ &\quad - \frac{73.5 \times 10^{-3}}{3000}\ (\text{m}) \\ &= 0.917\ \text{mm}, \end{aligned} \tag{26}$$

where $\mu_0 = 4\pi \times 10^{-7}$ H/m is the free-space permeability.

Here, we consider the fringing effect. The fundamental theory of the fringing effect is given in Appendix A. Here we assume the ratio of the effective width of the fringing flux cross-sectional area w_f, which is given in Fig. 5(b) in Appendix A, to the gap length as $u = w_f/l_g = 1$, and the ratio of the effective magnetic path length of the fringing flux to the gap length $k = 2$. From (66), the fringing flux factor F_f is

$$\begin{aligned} F_f &= 1 + \frac{2ul_g(C+F+2ul_g)}{kCF} \\ &= 1 + 2 \times 1 \times 0.917 \times 10^{-3} \\ &\quad \times \frac{(6.35 + 6.35 + 2 \times 1 \times 0.917)}{2 \times (6.35 + 6.35)} = 1.33. \end{aligned} \tag{27}$$

The number of turns N should be kept for achieving the specified K_u. From (62) in Appendix A, we obtain a new gap length for $N = 102$ and $F_r = 1.33$ as

$$\begin{aligned} l_g &= \frac{\mu_0 A_c F_f}{L}\left(N^2 - \frac{Ll_c}{\mu_0 \mu_r A_c}\right) \\ &= \frac{4 \times \pi \times 10^{-7} \times 40.1 \times 10^{-6} \times 1.33}{557 \times 10^{-7}} \\ &\times \left(102^2 - \frac{557 \times 10^{-7} \times 73.5 \times 10^{-3}}{4 \times \pi \times 10^{-7} \times 3000 \times 40.1 \times 10^{-6}}\right) \text{ (m)} \\ &= 1.22 \text{ mm}. \end{aligned} \tag{28}$$

We go to (27) again and iterative calculations between (27) and (28) are carried out until both l_g and F_f are converged. Fringing factor F_f and the gap length l_g are converged by eight iterations, which are $F_f = 1.56$ and $l_g = 1.43$ mm, respectively. We shall choose a standard value of the air-gap length $l_g = 1.4$ mm. Therefore, the estimated value of the inductance L_0 is

$$\begin{aligned} L_0 &= \frac{\mu_0 A_c N^2}{l_g/F_f + l_c/\mu_r} \\ &= \frac{4 \times \pi \times 10^{-7} \times 40.1 \times 10^{-6} \times 102^2}{1.4 \times 10^{-3}/1.56 + 73.5 \times 10^{-3}/3000} \\ &= 557 \ \mu\text{H}, \end{aligned} \tag{29}$$

which is exactly the same as the specified value.

From the height of the bobbin, we can obtained the maximum number of turns per one layer N' is

$$\begin{aligned} N\text{'} &= \frac{H}{d_o} \\ &= \frac{20.57}{0.785} = 26.2 \text{ turns/layer}. \end{aligned} \tag{30}$$

Therefore, the number of the winding layers N_l is

$$\begin{aligned} N_l &= \frac{N}{N\text{'}} \\ &= \frac{102}{26} = 3.92. \end{aligned} \tag{31}$$

We need 4-layer windings to realize the inductor. Because the wire length per single turn is

$$\begin{aligned} l_T &= C + 2E + F \\ &= 6.35 + 2 \times 18.8 + 6.35 \text{ (mm/turn)} \\ &= 4.98 \text{ cm/turn}, \end{aligned} \tag{32}$$

The length of the winding wire is

$$\begin{aligned} l_w &= Nl_T \\ &= 102 \times 4.98 \times 10^{-2} = 5.08 \text{ m}. \end{aligned} \tag{33}$$

The low-frequency winding resistance, which is almost equal to the dc winding resistance, is

$$\begin{aligned} R_{wdc} &= \frac{\rho_w l_w}{A_w} \\ &= \frac{1.72 \times 10^{-8} \times 5.08}{0.411 \times 10^{-6}} = 0.213 \ \Omega, \end{aligned} \tag{34}$$

where $\rho_w = 1.72 \times 10^{-8}$ Ωm is the resistivity of the copper at T =20 °C. The dc winding power loss without the skin and proximity effects is

$$\begin{aligned} P_{wdc} &= \frac{R_{wdc} I_m^2}{2} \\ &= \frac{0.215 \times 1.51^2}{2} = 0.242 \text{ W}. \end{aligned} \tag{35}$$

The skin depth of copper at $f = 100$ kHz is

$$\begin{aligned} \delta_w &= \frac{\rho_w}{\pi \mu_0 f} \\ &= \sqrt{\frac{1.724 \times 10^{-8}}{\pi \times 4 \times \pi \times 10^{-7} \times 100 \times 10^3}} \text{ (m)} \\ &= 0.209 \text{ mm}. \end{aligned} \tag{36}$$

We estimate the ac winding loss using Dowell's equation. The factor of Dowell's equation for round wire, which is obtained from (84) as shown in Appendix B, is

$$\begin{aligned} A &= \left(\frac{\pi}{4}\right)^{\frac{3}{4}} \frac{d}{\delta_w}\sqrt{\frac{dN\text{'}}{H}} \\ &= \left(\frac{\pi}{4}\right)^{\frac{3}{4}} \frac{0.723}{0.209}\sqrt{\frac{0.723 \times 26}{20.57}} = 2.76. \end{aligned} \tag{37}$$

By using $A = 2.76$ and (70) in Appendix B, we obtain the winding ac-to-dc resistance ratio

$$\begin{aligned} F_R &= A\left[\frac{\sinh(2A) + \sin(2A)}{\cosh(2A) - \cos(2A)}\right. \\ &\quad \left. + \frac{2(N_l^2 - 1)}{3}\frac{\sinh(A) - \sin(A)}{\cosh(A) + \cos(A)}\right] \\ &= 2.76\left[\frac{\sinh(2 \times 2.76) + \sin(2 \times 2.76)}{\cosh(2 \times 2.76) - \cos(2 \times 2.76)}\right. \\ &\quad \left. + \frac{2(4^2 - 1)}{3}\frac{\sinh(2.76) - \sin(2.76)}{\cosh(2.76) + \cos(2.76)}\right] \\ &= 32.3. \end{aligned} \tag{38}$$

The high-frequency ac resistance is

$$\begin{aligned} R_{wac} &= F_R R_{wdc} \\ &= 32.3 \times 0.213 = 6.87 \ \Omega. \end{aligned} \tag{39}$$

Therefore, the high-frequency ac winding power loss is

$$\begin{aligned} P_{wac} &= F_R P_{wdc} \\ &= 32.3 \times 0.242 = 7.83 \text{ W}. \end{aligned} \tag{40}$$

The core power loss per unit volume at $f = 100$ kHz is

$$\begin{aligned} P_v &= 0.0573 \times f^{1.66} \times (10 \times B_m)^{2.68} \\ &= 0.0573 \times 100^{1.66} \times (10 \times 0.206)^{2.68} \\ &= 830 \text{ mW/cm}^3. \end{aligned} \tag{41}$$

The total core loss is

$$\begin{aligned} P_c &= P_v V_c \\ &= 830 \times 10^{-3} \times 2.95 = 2.45 \text{ W}. \end{aligned} \tag{42}$$

The equivalent series resistance (ESR) for core loss is expressed

$$\begin{aligned} R_c &= \frac{2P_c}{I_m^2} \\ &= \frac{2 \times 2.45}{1.51^2} = 2.15 \ \Omega. \end{aligned} \tag{43}$$

Therefore, the total power loss in the inductor is

$$\begin{aligned} P_{cw} &= P_c + P_{wac} \\ &= 2.45 + 7.83 = 10.3 \text{ W}. \end{aligned} \tag{44}$$

The equivalent series resistance of the inductor is

$$\begin{aligned} R_{esr} &= R_{wac} + R_c \\ &= 6.87 + 2.15 = 9.02 \ \Omega. \end{aligned} \tag{45}$$

The quality factor of the inductor is

$$\begin{aligned} Q &= \frac{\omega L}{R_{esr}} \\ &= \frac{2 \times \pi \times 10^3 \times 557 \times 10^{-6}}{9.02} = 38.8. \end{aligned} \tag{46}$$

B. Multiple-Strand Winding

The design in this section illustrates how we can reduce the skin and proximity effects using a multi-strand wire. For this purpose, the diameter of a single strand should be

$$\begin{aligned} d_s &< 2\delta_w \\ &= 2 \times 0.209 \times 10^{-3} \text{ (m)} = 0.418 \text{ mm}. \end{aligned} \tag{47}$$

The closest wire is AWG 26 with the bare wire diameter $d_s = 0.405$ mm, the insulated wire diameter $d_{so} = 0.452$ mm, and the bare wire cross-sectional area $A_{ws} = 0.128$ mm^2. The number of strands is

$$\begin{aligned} N_s &= \frac{A_w}{A_{ws}} \\ &= \frac{0.378}{0.128} = 2.95. \end{aligned} \tag{48}$$

The number of strands $N_s = 3$ is selected. From (5), the number of turns is

$$\begin{aligned} N &= \frac{K_u W_a}{A_w} \\ &= \frac{K_u W_a}{\pi d_s^2 N_s / 4} \\ &= \frac{0.4 \times 104.7 \times 10^{-6}}{\pi \times (0.405 \times 10^{-3})^2 \times 3/4} = 108.3. \end{aligned} \tag{49}$$

Following the iterative calculations between (27) and (28), we can obtain fringing factor $F_f = 1.72$ and gap length $l_g = 1.77$ mm. Therefore, we determine the gap length is $l_g = 1.8$ mm. In this case, the designed inductance value is $L_0 = 557$ μH.

The wire length is $l_w = 5.38$ m following the same procedure in (26) and (33). The low-frequency winding resistance is

$$\begin{aligned} R_{wdc} &= \frac{\rho_w l_w}{N_s A_{ws}} \\ &= \frac{1.72 \times 10^{-8} \times 5.38}{3 \times 0.128 \times 10^{-6}} = 0.241 \ \Omega. \end{aligned} \tag{50}$$

The low-frequency winding loss is

$$\begin{aligned} P_{wdc} &= \frac{R_w I_m^2}{2} \\ &= \frac{0.241 \times 1.53^2}{2} = 0.274 \text{ W}. \end{aligned} \tag{51}$$

Because of using the multiple strands, the skin and proximity effects can be ignored. Therefore, the total loss in the inductor is

$$\begin{aligned} P_{cw} &= P_c + P_{wdc} \\ &= 2.45 + 0.27 = 2.72 \text{ W}. \end{aligned} \tag{52}$$

The ESR of the inductor with multiple strands is

$$\begin{aligned} R_{esr} &= R_{wdc} + R_c \\ &= 0.24 + 2.15 = 2.39 \ \Omega. \end{aligned} \tag{53}$$

The quality factor of the inductor for multi-strand winding is

$$\begin{aligned} Q &= \frac{\omega L}{R_{esr}} \\ &= \frac{2 \times \pi \times 10^3 \times 557 \times 10^{-6}}{2.39} = 146. \end{aligned} \tag{54}$$

Comparing (54) with (46), it is seen that the multi-strand winding provides 3.8 % times as high quality fator as single-wire winding.

IV. Discussion of A_p Method Applicability

Since a high-frequency current generates a large power loss due to the skin and proximity effects, the multiple-strand winding is a good solution for high efficiency. By using the multiple-strand winding, it is seen that the core losses are larger than winding losses, which is an important difference between resonant inductors and CCM/DCM inductors for buck converters. The theory of the area product method is based on the assumption of low core loss. For low core-loss case, the amplitude of the magnetic flux density B_m is limited by the saturated flux density B_s. In the example of Section III, we selected the initial value of maximum flux density B_m is $B_m = 0.2$ T. This value comes from a typical value of saturated flux density $B_s = 0.4$ T with a sufficient margin at T_{max} in core temperature.

Note that the value of A_p is independent of the frequency of the current, but the core power loss strongly depends on the frequency strongly. Suppose that the design specifications of the frequency is changed from $f = 100$ Hz to $f = 1$ MHz.

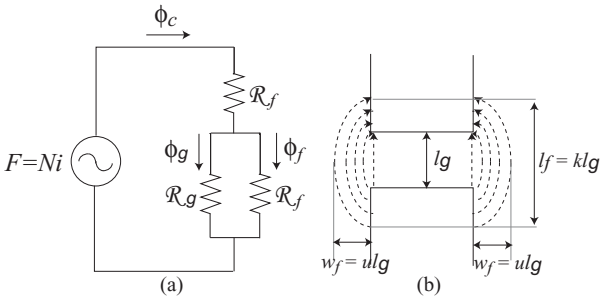

Fig. 5. Illustration for the fringing-effect explanation. (a) Magnetic equivalent circuit of an inductances with an air gap and a fringing magnetic flux. (b) The relationship between gap length l_g, mean effective of the magnetic path length in the fringing area l_f and effective width of the fringing flux cross-sectional area w_f.

In this case, we select the same core as that for $f = 100$ Hz following the same procedure of the design example. However, the core loss becomes 52 times larger, which is not acceptable from a point of view of the efficiency. In this case, it is necessary to reset a lower B_m or another material with lower μ_r, which requires trial-and-error efforts.

The problem of large loss occurs when the high-frequency and large-swing of current flows through the inductor. The high-frequency resonant inductor is a typical case of it. From these discussions, we can conclude that the A_p method is very effective to design the resonant inductor with low frequency and small amplitude of the current. However, the assumption of B_m is a big problem for the resonant-inductor design with high frequency and large amplitude of the flux density B_m.

V. Conclusion

This paper has presented the expressions of the area product for resonant inductors. By using the proposed expressions, we can determine the area-product value from loaded quality factor, output power, and operating frequency assuming the window utilization factor K_u and the maximum flax density B_m. The results of design example in this paper indicate that it is very important to check the core loss carefully when the resonant inductor is designed. We have shown that the total winding loss can be reduced by using multiple-strand winding.

Appendix

A. Fringing Flux Effect on Inductance and Number of Turns

A fringing flux is present around the air gap whenever the core is excited. The magnetic flux lines bulge outward because the magnetic lines repel each other when passing through a nonmagnetic material. As a result, the cross-sectional area of the magnetic field is increased and the flux density is decreased. This effect is called the fringing flux effect. The percentage of the fringing flux in the total magnetic flux increase as the air gap length l_g increases. The maximum increase in the radius of the magnetic flux due to the fringing effect is approximately equal to the length of the air gap l_g. Fig. 5(a) shows a magnetic equivalent circuit for the inductor with a single air gap and a fringing flux. The fringing permeance is shunting the gap permeance.

Due to the continuity of the magnetic flux, the magnetic flux in the core ϕ_c is equal to the sum of the magnetic flux in the air gap ϕ_g and the fringing flux ϕ_f

$$\phi_c = \phi_g + \phi_f. \tag{55}$$

The permeance of the core is

$$\mathcal{P}_c = \frac{1}{\mathcal{R}_c} = \frac{\mu_r \mu_0 A_c}{l_c}. \tag{56}$$

The permeance of the air gap is

$$\mathcal{P}_g = \frac{1}{\mathcal{R}_g} = \frac{\mu_0 A_c}{l_g}. \tag{57}$$

The permeance of the fringing area is

$$\mathcal{P}_f = \frac{1}{\mathcal{R}_f} = \frac{\mu_0 A_f}{l_f}, \tag{58}$$

where A_f is the fringing area and l_f is mean effective of the magnetic path length in the fringing area as shown in Fig. 5(b).

The total permeance of the air gap and the fringing area is

$$\begin{aligned} \mathcal{P}_{gf} &= \mathcal{P}_g + \mathcal{P}_f = \mathcal{P}_g \left(1 + \frac{\mathcal{P}_f}{\mathcal{P}_g}\right) \\ &= \frac{\mu_0 A_c}{l_g} + \frac{\mu_0 A_f}{l_f} = \frac{\mu_0 A_c F_f}{l_g}, \end{aligned} \tag{59}$$

where F_f is the fringing factor, which is expressed as

$$F_f = \frac{\mathcal{P}}{\mathcal{P}_g} = 1 + \frac{\mathcal{P}_f}{\mathcal{P}_g} = 1 + \frac{A_f l_g}{A_c l_f} = 1 + \frac{A_f}{A_c k}, \tag{60}$$

where $k = l_f / l_g$ is the ratio of mean effective of the magnetic path length in the fringing area to the gap length. The total reluctance of the inductor is

$$\begin{aligned} \mathcal{R} &= \mathcal{R}_c + \mathcal{R}_g || \mathcal{R}_f = \mathcal{R}_c + \frac{1}{\mathcal{P}_{gf}} \\ &= \frac{l_c}{\mu_r \mu_0 A_c} + \frac{l_g}{\mu_0 A_c F_f} = \frac{l_g}{\mu_0 A_c} \left(\frac{l_c}{\mu_r l_g} + \frac{1}{F_f}\right). \end{aligned} \tag{61}$$

The inductance value including the fringing effect is

$$L = \frac{N^2}{\mathcal{R}} = \frac{\mu_0 A_c N^2}{l_g / F_f + l_c / \mu_r}. \tag{62}$$

A-1. Fringing Flux Factor for Rectangular Air Gap

Consider a core with a single rectangular air gap. The ratio of the mean width of the cross-sectional area of the fringing flux to the air gap length is defined as

$$u = \frac{w_f}{l_g}. \tag{63}$$

By using the E-core model shown in Fig. 4, the cross-sectional area of the air gap is

$$A_c = CF. \tag{64}$$

The cross-sectional area of the fringing flux is

$$A_f = (C + 2ul_g)(F + 2ul_g) - CF = 2ul_g(C + F + 2ul_g). \tag{65}$$

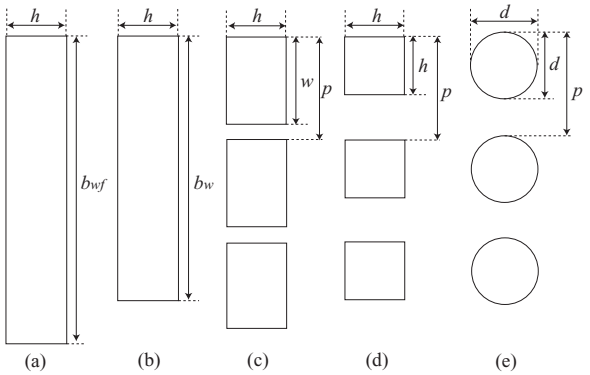

Fig. 6. Transformation of a foil winding to rectangular, square, and round wire windings. (a) Wide foil winding. (b) Narrow foil winding. (c) Rectangular winding conductor. (d) Square winding conductor. (e) Round winding wire.

Substituting (64) and (65) into (60), the fringing flux factor for a rectangular air gap is

$$F_R = 1 + \frac{A_f}{A_c k} = 1 + \frac{2ul_g(C + F + 2ul_g)}{kCF}. \quad (66)$$

A-2. Fringing Flux Factor for Round Air Gap

In case of a round core case, the cross-sectional area of a round air gap with diameter D_c is

$$A_c = \frac{\pi D_c^2}{4}. \quad (67)$$

The cross-sectional area of the fringing flux for a round air gap is

$$A_f = \frac{\pi(D_c + 2ul_g)^2}{4} - \frac{\pi D_c^2}{4} = \pi u l_g (D_c + u l_g). \quad (68)$$

Substituting (67) and (68) into (60), the fringing flux factor for a round air gap is

$$F_R = 1 + \frac{A_f}{A_c k} = 1 + \frac{4ul_g(D_c + ul_g)}{kD_c^2}. \quad (69)$$

B. Dowell's Equation for Round Wire

The skin and proximity effect factor, which is the winding ac-to-dc resistance ratio given by Dowell's equation for a (ideally, infinitely wide) foil winding with a single turn per layer, using a one-dimensional model [10], is given by

$$\begin{aligned} F_R &= \frac{R_{wac}}{R_{wdc}} \\ &= A\left[\frac{\sinh(2A) + \sin(2A)}{\cosh(2A) - \cos(2A)} \right. \\ &\quad \left. + \frac{2(N_l^2 - 1)}{3} \frac{\sinh(A) - \sin(A)}{\cosh(A) + \cos(A)}\right]. \end{aligned} \quad (70)$$

Equation (70) derived for the winding with a single wide foil per layer can be extended to other winding shapes, such as rectangular, square, and round winding conductors to obtain approximate analytical descriptions of the winding resistance. A porosity factor can be introduced when converting one sheet of a foil conductor into several equivalent conductors in each layer to ensure that the dc resistance of the windings remains unchanged. A transformation of foil winding to various shapes of a winding conductor is illustrated in Fig. 6(a). A sheet of a foil shown in Fig. 6(a) is first replaced by a narrow sheet of a foil as depicted in Fig. 6(b). Next the narrow sheet of foil is replaced by several rectangular conductors, as shown in Fig. 6(c). Then the rectangular conductors are replaced with square conductors depicted in Fig. 6(d). Finally, the square conductors are replaced by round conductors in Fig. 6(e).

The procedure for transforming a rectangular winding conductor is as follows. Consider two foil windings with a single turn per layer. Both foil windings have the same length l_w and thickness h. However, the widths and the resistivities of the foils are different. The wider foil has the width (or the winding breadth) b_{wf} and the resistivity $\rho_{wf} > \rho_w$. Consequently, the narrow conductor skin depth δ_w is lower than the wide conductor skin depth δ_{wf}, i.e., $\delta_w < \delta_{wf}$. The resistivities are such that the dc resistances of both windings remain the same. The dc resistance of the wide foil winding is given by

$$R_{dcf} = \frac{\rho_{wf} l_w}{h b_{wf}}, \quad (71)$$

and the dc resistance of the narrow foil winding is

$$R_{dc} = \frac{\rho_w l_w}{h b_w}. \quad (72)$$

The narrow foil is cut into rectangular conductors of width w and stretched so that each layer has N_{tl} turns, the width of each conductor is

$$w = \frac{b_w}{N_{tl}}, \quad (73)$$

and the distance between the centers of two adjacent conductors, called the winding pitch, is defined by

$$p = \frac{b_{wf}}{N_{tl}}. \quad (74)$$

As mentioned, the dc resistance of both foil windings are the same $R_{dc} = R_{dcf}$. Thus,

$$\frac{\rho_w l_w}{h b_w} = \frac{\rho_{wf} l_w}{h b_{wf}}, \quad (75)$$

which gives the ratio of two resistivities

$$\frac{\rho_w}{\rho_{wf}} = \frac{b_w}{b_{wf}} = \frac{w N_{tl}}{p N_{tl}} = \frac{w}{p} = \eta, \quad (76)$$

where the layer porosity factor is defined as

$$\eta = \frac{w}{p}. \quad (77)$$

The minimum distance between the turns of the same layer is determined by the thickness of the winding conductor insulation

$$g_{min} = p_{min} - w. \quad (78)$$

Hence, the maximum porosity factor is

$$\eta_{max} = \frac{w}{p_{min}} = \frac{w}{w + g_{min}} = \frac{1}{1 + g_{min}/w}. \quad (79)$$

The ratio of the skin depths is given by

$$\frac{\delta_w}{\delta_{wf}} = \sqrt{\frac{\rho_w}{\rho_{wf}}} = \sqrt{\frac{w}{p}} = \sqrt{\eta}. \tag{80}$$

In summary, the layer porosity factor $\eta = b_w/b_{wf}$ is modeled by a decrease in the resistivity of the multiple-turn layer $\rho_w = \eta\rho_{wf} = (w/p)\rho_{wf}$. The reduced resistivity causes a decrease in the skin depth of the multi-turn layer $\delta_w = \sqrt{\eta}\delta_{wf}$, reducing the value of $A = \sqrt{\eta}h/\delta_w$. At high frequencies, the layer porosity factor η gives a good approximation only for high values of η when conductors are closely packed [11], [12].

B-1: Rectangular Winding Conductor

For a rectangular wire winding shown in Fig. 6(c),

$$A = A_r = \frac{h}{\delta_{wf}} = \frac{h}{\delta_w}\sqrt{\frac{w}{p}} = \frac{h}{\delta_w}\sqrt{\eta_r}, \tag{81}$$

where h is the conductor height, w is the conductor width, p is the distance between the centers of two adjacent conductors called the winding pitch, and $\eta_r = w/p$ is the porosity factor.

B-2: Square Winding Conductor

For a square wire winding shown in Fig. 6(d), $w = h$. Hence, (81) becomes

$$A = A_s = \frac{h}{\delta_w}\sqrt{\frac{h}{p}} = \frac{h}{\delta_w}\sqrt{\eta_s}, \tag{82}$$

where $\eta_s = h/p$ is the porosity factor.

B-3: Round Winding Wire

To adopt (70) for a round wire winding shown in Fig. 6(e), a round conductor can be approximated by a square conductor of the same cross-sectional area. This approach guarantees that the dc resistance of the round and square conductors remain unchanged. The relationship between h and the effective round wire diameter d under the conditions of the same cross-sectional area is

$$h = \frac{d\sqrt{\pi}}{2}. \tag{83}$$

Note that if the square and round wire areas are the same, the dc resistances of both windings are the same. By substituting (83) into (82) gives

$$A = A_o = \frac{h}{\delta_w}\sqrt{\frac{h}{p}} = \left(\frac{\pi}{4}\right)^{\frac{3}{4}}\frac{d}{\delta_w}\sqrt{\frac{d}{p}} = \left(\frac{\pi}{4}\right)^{\frac{3}{4}}\frac{d}{\delta_w}\sqrt{\eta_o}, \tag{84}$$

where $\eta_o = d/p$ is the porosity factor, which is the same as (37).

For high-frequency case, the value of A_o becomes large since the skin depth δ_w becomes small. With numerical plots, it is seen that

$$\frac{\sinh(2A)+\sin(2A)}{\cosh(2A)-\cos(2A)} \approx \frac{\sinh(A)-\sin(A)}{\cosh(A)+\cos(A)} \approx 1, \quad \text{for } A_o > 2.5. \tag{85}$$

By using this approximation, (70) is rewritten as

$$F_R \approx A_o\frac{2N_l^2+1}{3}, \quad \text{for } A_o > 2.5, \tag{86}$$

which is approximate expression of Dowell's equation for high frequencies.

REFERENCES

[1] W. G. Hurley, W. H. Wolfle, and J. G. Bereslin, "Optimized transformer design: Inclusive of high-frequency effects," *IEEE Trans. Power Electron.* vol. 13, no. 4, pp. 651–659, July 1998.

[2] K. W. E. Cheng and P. D. Evans, "Calculation of winding losses in high frequency toroidal inductors using multistrand conductors," *IEE-B, Electric Power Applications,* vol. 142, no. 5, pp. 313–322, Sept. 1995.

[3] W. A. Roshen, L. Steierwald, R. J. Charles, W. G. Earls, and C. F. Saj, "High-efficiency, high-density MHz magnetic components for low profile converters," *IEEE Trans. Industry Appl.*, vol. 31, no. 4, pp. 869 – 878, July/Aug. 1995.

[4] H. Sheng, Y. Pei, and F. Wang, "Impact of resonant tank structures on transformer size for a high power density isolated resonant converter," *2008 IEEE Power Electronics Specialists Conference (PESC 2008)*, Rhodes, Greece, June 2008, pp. 2975 – 2981.

[5] H. Njiende, N. Frohleke, and J. Bocker, "Optimized size design of integrated magnetic components using area product approach," *2005 European Conference on Power Electronics and Applications (EPE 2005)*, Dresden, Germany, Sept. 2005, pp. 1 – 10.

[6] N. Ekekwe, J. E. Ndubah, K. White, and O. B. Oni, "Practical process in high frequency distribution transformer design," *Proceedings of 2003 Electrical Insulation Conference and Electrical Manufacturing & Coil Winding Technology Conference*, Indianapolis, USA, Sept. 2003, pp. 121 – 128.

[7] C. W. T. McLyman, *Transformer and Inductor Design Handbook,* 3rd Ed., New York, NY: Marcel Dekker, 2004.

[8] C. W. T. McLyman, *Magnetic Core Selection for Transformer and Inductors,* 2nd Ed., New York, NY: Marcel Dekker, 1997.

[9] Magnetics Inc., *Ferrite Cores*, 2006.

[10] P. J. Dowell, "Effects of eddy currents in transformer winding," *Proc. IEE,* vol. 113, no. 8, pp. 1387–1394, Aug. 1966.

[11] E. C. Snelling, *Soft Ferrites: Properties and Applications,* London: Iliffe Books Ltd, 1969.

[12] F. Robert, "A theoretical discussion about the layer copper factor used in winding loss calculation," *IEEE Trans. Magnetics,* vol. 38, no. 5, pp. 3177 – 3179, Sept. 2002.